

QCDLAB: Designing Lattice QCD Algorithms with MATLAB

Artan Boriçi

Physics Department, University of Tirana

Bld. King Zog I, Tirana-Albania

borici@fshn.edu.al

Abstract

This paper introduces QCDLAB, a design and research tool for lattice QCD algorithms. The tool, a collection of MATLAB functions, is based on a “small-code” and a “minutes-run-time” algorithmic design philosophy. The present version uses the Schwinger model on the lattice, a great simplification, which shares many features and algorithms with lattice QCD. A typical computing project using QCDLAB is characterised by short codes, short run times, and the ability to make substantial changes in a few seconds. QCDLAB 1.0 can be downloaded from the QCDLAB project homepage <http://phys.fshn.edu.al/qcdlab.html>.

arXiv:hep-lat/0610054v1 9 Oct 2006

Contents

1	Advancement of Lattice QCD	2
2	Simulation of lattice QCD	3
3	Foundations of Krylov Subspace Methods	6
4	QCDLAB 1.0	9
4.1	Simulation Algorithms	9
4.2	Inversion Algorithms	15
4.3	Ginsparg-Wilson Fermions	20
5	QCDLAB 2.x	23

1 Advancement of Lattice QCD

Lattice QCD, an industrial-range computing project, is in its fourth decade. It has basically two major computing problems: simulation of QCD path integral and calculation of quark propagators. Generally, these problems lead to very intensive computations and require high-end computing platforms.

However, we wish to make a clear distinction between lattice QCD test and production codes. This is very important in order to develop a compact and easily manageable computing project. While this is obvious in theory, it is less so in lattice QCD practicing: those who write lattice codes are focused primary on writing production codes. What is usually called test code is merely a test of production codes.

The code of a small project is usually small, runs fast, it is easy to access, edit and debug. Can we achieve these features for a lattice test code? Or, can we modify the goals of the lattice project in order to get such features? In our opinion, this is possible for a *minimal test code*, a test code consisting of a minimal possible code which is able to test gross features of the theory and algorithms at shortest possible time and largest acceptable errors on a standard computing platform. This statement needs more explanation:

- a. Although it is hard to give sharp constraints on the number of lines of the test code, we would call “minimal” that code which is no more than a few printed pages.
- b. The run time depends on computing platforms and algorithms, and the choice of lattice action and parameters. It looks like a great number of degrees of freedom here, but in fact there are hardly good choices in order to reduce the run time of a test code without giving up certain features of the theory. Again, it is tremendously difficult to give run times. However, a “short” run time should not exceed a few minutes of wall-clock time.
- c. We consider a computing platform as being “standard” if its cost is not too high for an academic computing project.
- d. We call simulation errors to be the “largest acceptable” if we can distinguish clearly signal from noise and when gross features of the theory are not compromised by various approximations or choices.
- e. Approximations should not alter basic features of the theory. The quenched approximation, for example, should not be considered as an acceptable approximation when studying QCD with light quarks.

A test code with these characteristics should *signal the rapid advance in the field*, in which case, precision lattice computations are likely to happen in many places around the world. Writing a minimal test code is a *challenge of three smarts*: smart computers, smart languages and smart algorithms.

In this paper we introduce the first version of QCDLAB, QCDLAB 1.0, a collection of MATLAB functions for the simulation of lattice Schwinger model. This is part of a larger project for algorithmic development in lattice QCD. It can be used as a small laboratory to test and validate algorithms. In particular, QCDLAB 1.0 serves as an illustration of the minimal test code concept.

QCDLAB can also be used for newcomers in the field. They can learn and practice lattice projects which are based on short codes and run times. This offers a “learning by doing” method, perhaps a quickest route into answers of many unknown practical questions concerning lattice QCD simulations.

The next two sections describe basic algorithms for simulation of lattice QCD and foundations of Krylov subspace methods. Then, we present the QCDLAB 1.0 functions followed by examples of simple computing projects. The last section outlines the future plans of the QCDLAB project.

2 Simulation of lattice QCD

Notations and Problem definition

Lattice gauge fields $U_{\mu,i}$, our basic degrees of freedom, are defined on oriented links $i \rightarrow i + \hat{\mu}$ of a four dimensional hypercubic lattice with N sites and lattice spacing a . Here, i is a four component index labeling the lattice sites, $\mu = 1, 2, 3, 4$ labels directions in the Euclidean space, and $\hat{\mu}$ is the unit vector along μ -direction. Algebraically, a lattice gauge field is an order 3, complex valued unitary matrix with determinant one, an element of the $SU(3)$ colour group.

The basic computational task in lattice QCD is the generation of ensembles of gauge field configurations according to probability density:

$$\rho_{QCD}(U) \sim \det(D^* D) e^{-S_g(U)},$$

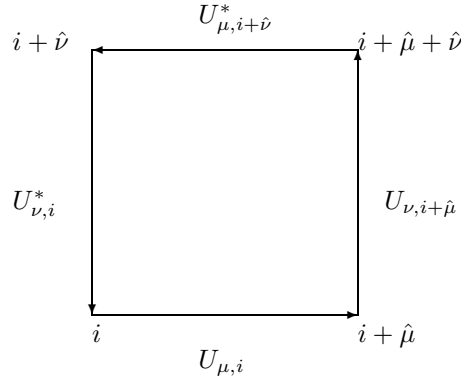
where D is the lattice Dirac operator,

$$S_g = \beta \operatorname{Re} \sum_{i, \mu < \nu} (1 - P_{\mu\nu,i})$$

is the gauge action, $\beta = 6/g^2$ is the gauge-boson coupling constant, and

$$P_{\mu\nu,i} = \frac{1}{3} \operatorname{tr} U_{\mu,i} U_{\nu,i+\hat{\mu}} U_{\mu,i+\hat{\nu}}^* U_{\nu,i}^*$$

is the *plaquette* in $\mu\nu$ plane, a 4-link product defined as in the figure.



We have assumed here a fermion theory with two degenerate flavours of quark masses which suffices for the purpose of this paper. There are two main formulations of lattice fermions: Wilson [1] and Kogut-Susskind [2], called also staggered, discretizations of the Dirac operator. Wilson operator, linking sites i and j , is given by

$$D_{ij} = (m + \frac{4}{a}) I_4 \otimes I_3 \delta_{ij} - \frac{1}{2} \sum_{\mu} [(I_4 - \gamma_{\mu}) \otimes U_{\mu,i} \delta_{i,j+\hat{\mu}} + (I_4 + \gamma_{\mu}) \otimes U_{\mu,i-\hat{\mu}} \delta_{i,j-\hat{\mu}}],$$

whereas Kogut-Susskind operator is given by

$$D_{ij} = m I_3 \delta_{ij} + \frac{1}{2} \sum_{\mu} (-1)^{i_1 + \dots + i_{\mu-1}} (U_{\mu,i} \delta_{i,j+\hat{\mu}} - U_{\mu,i-\hat{\mu}} \delta_{i,j-\hat{\mu}}).$$

Here m is the bare quark mass, γ_{μ} are anticommuting Hermitian *gamma-matrices* acting on Dirac space

$$\gamma_{\mu} \gamma_{\nu} + \gamma_{\nu} \gamma_{\mu} = 2 \delta_{\mu\nu} I_4,$$

and \otimes denotes the direct or Kronecker product of matrices. Hence, Wilson and Kogut-Susskind operators are complex valued matrices of order $12N$ and $3N$ with $49N$ and $25N$ nonzero elements respectively.

Note that the difficulty of handling the determinant of a huge matrix can be softened using the Gaussian integral expression:

$$\det(D^* D) = \int \prod_{i=1}^N \frac{d\operatorname{Re}(\phi_i) d\operatorname{Im}(\phi_i)}{\pi} e^{-\phi^* (D^* D)^{-1} \phi} \quad (2.1)$$

where ϕ is a complex valued field, a *psudofermion* field. Thus, the determinant is traded for the inversion. All we need now is to generate ensembles according to the new density:

$$\rho_{QCD}(U, \phi) \sim \exp\{-S_g(U) - \phi^* (D D^*)^{-1} \phi\}.$$

Hybrid Monte Carlo Algorithm

The HMC algorithm [3] starts by introducing $su(3)$ conjugate momenta P to $SU(3)$ lattice gauge fields. Hence, the classical Hamiltonian can be written in the form

$$\mathcal{H}(P, U, \phi) = \frac{1}{2} \text{tr} P^2 + S_g(U) + \phi^* (DD^*)^{-1} \phi ,$$

whereas expanded probability density is

$$\hat{\rho}_{QCD}(P, U, \phi) \sim \exp\{\mathcal{H}(P, U, \phi)\} .$$

The idea of the HMC algorithm is as follows:

- i) Use global heatbath for pseudofermion field update. If ζ is a Gaussian pseudofermion field, the new field is updated according to the equation

$$\phi = D\zeta .$$

- ii) Integrate numerically classical equations of motion.
- iii) Correct numerical integration error using Metropolis *et al* algorithm.

Classical Equations of Motion

The first first equation of motion is defined using conjugate momenta:

$$\dot{U}_{\mu,i} = iP_{\mu,i} U_{\mu,i} .$$

For the second equation one writes down the total derivative of the Hamiltonian:

$$\dot{\mathcal{H}} = \sum_{\mu,i} \text{tr} P_{\mu,i} \dot{P}_{\mu,i} + \dot{S}_g - \phi^* (DD^*)^{-1} \dot{D} D^* (DD^*)^{-1} \phi + h.c. ,$$

Substituting for $\dot{U}_{\mu,i}$ the first equation of motion and using

$$\dot{\mathcal{H}} = 0 ,$$

one finds the second equation of motion

$$\dot{P}_{\mu,i} = F_{\mu,i} .$$

From $\dot{\mathcal{H}}$ expression, it is clear that in order to evaluate the force $F_{\mu,i}$, one must calculate $(DD^*)^{-1} \phi$.

Leapfrog Algorithm

The widely used algorithm for solving equations of motions is the leapfrog algorithm

$$\begin{aligned} Q_{\mu,i} &= P_{\mu,i} + F_{\mu,i} \frac{\Delta t}{2} \\ U'_{\mu,i} &= e^{iQ_{\mu,i} \Delta t} U_{\mu,i} \\ P'_{\mu,i} &= Q_{\mu,i} + F'_{\mu,i} \frac{\Delta t}{2} , \end{aligned}$$

where the primed fields are those advanced by Δt and $Q_{\mu,i}$ are half-step momenta. The algorithm starts at $t = 0$, where momenta are taken to be Gaussian noise. Then it continues up to time $t = \tau$ for $N_{\text{mic}} = \tau/\Delta t$ number of steps.

It is easy to show that this scheme is reversible and preserves infinitesimal area of the phase space. Reversibility guarantees detailed balance of HMC, whereas area preservation ensures that there are no corrections due to integration measure. However, Hamiltonian is not conserved since

$$H' - H = \frac{1}{2} \ddot{H} \Delta t^2 + O(\Delta t^3) .$$

Metropolis *et al* Algorithm

The HMC algorithm ends up accepting or rejecting the proposed gauge field $\{U_{\mu,i}(\tau)\}$ using Metropolis *et al* algorithm [4]. The acceptance probability for this algorithm is

$$P_{\text{acc}}(\{P(0), U(0)\} \rightarrow \{P(\tau), U(\tau)\}) = \min \left\{ 1, e^{H(\tau) - H(0)} \right\}$$

On rejection, one goes back to time $t = 0$ and refreshes momenta.

Inversion Algorithms

Calculation of forces and quark propagators requires the solution of linear systems

$$Dx = b ,$$

where D is a the lattice Dirac operator and b the right hand side. As we noted earlier, D is a large and sparse matrix. For these matrices, *Krylov subspace methods* provide the most efficient inversion algorithms [5]. Such an algorithm is the Conjugate Gradients (CG) algorithm [6].

Conjugate Gradients

Given an approximation x_0 , the algorithm starts with computation of the *residual vector* r_0 ,

$$r_0 = b - Ax_0 ,$$

and initialisation of a vector p_0 to the starting residual, $p_0 = r_0$. Note that CG assumes that A is a *positive definite* and Hermitian matrix. Then, the algorithm iterates these vectors using recursions

$$\begin{aligned} x_{k+1} &= x_k + \alpha_k p_k \\ r_{k+1} &= r_k - \alpha_k A p_k \\ p_{k+1} &= r_{k+1} + \beta_{k+1} p_k , \end{aligned}$$

where

$$\alpha_k = \frac{r_k^* r_k}{p_k^* A p_k}, \quad \beta_{k+1} = \frac{r_{k+1}^* r_{k+1}}{r_k^* r_k} .$$

Conjugate Gradients on Normal Equations

Since the lattice Dirac operator is neither positive definite nor Hermitian one takes $A = D^* D$ and solves for the *normal equations*

$$D^* D x = D^* b .$$

Then, we get what we call the Conjugate Gradients algorithm on Normal Equations (CGNE). As with standard CG, given an approximation x_0 , the algorithm computes starting residual r_0 ,

$$r_0 = b - D x_0 ,$$

and initialises p_0 to r_0 . Additionally, a new vector s_0 is initialised using $s_0 = D^* r_0$. The CGNE algorithm recursions are

$$\begin{aligned} x_{k+1} &= x_k + \alpha_k p_k \\ r_{k+1} &= r_k - \alpha_k D p_k \\ p_{k+1} &= s_{k+1} + \beta_{k+1} p_k , \end{aligned}$$

where

$$s_{k+1} = D^* r_{k+1} ,$$

and

$$\alpha_k = \frac{s_k^* s_k}{(D p_k)^* (D p_k)}, \quad \beta_{k+1} = \frac{s_{k+1}^* s_{k+1}}{s_k^* s_k} .$$

A Convergence Result

It can be theoretically proven that CGNE algorithm converges *linearly*, i.e.

$$\|r_k\| \leq 2 \left(\frac{\kappa(D) - 1}{\kappa(D) + 1} \right) \|r_{k-1}\| ,$$

where $\|\cdot\|$ denotes the Euclidean norm and $\kappa(D)$ is the *condition number* of the Dirac operator. In terms of *singular values* of D , $\sigma_1 \geq \sigma_2 \geq \dots \geq \sigma_N$, the condition number is given by

$$\kappa(D) = \frac{\sigma_1}{\sigma_N} .$$

If D is rescaled such that $\sigma_1 = 1$ we get (see [5], p52)

$$\|r_k\| \leq 2 \left(\frac{1 - \sigma_N}{1 + \sigma_N} \right)^k \|r_0\| .$$

It can be shown that CGNE calculates a solution of the minimisation problem

$$\min_{x \in \mathbb{C}^N} \|b - Dx\| .$$

But for non-normal matrices, such as the Wilson-Dirac operator, this solution is *sub-optimal*. Unlike CGNE, the General Minimised Residual (GMRES) algorithm calculates the *optimal* solution of this problem. Both methods converge according to the law described above. However, σ_N is traded for the spectral gap, which is larger (for non-normal matrices). As we will show later, GMRES algorithm is more expensive and often prohibitive in terms of computer resources.

3 Foundations of Krylov Subspace Methods

A Krylov subspace is the space built from the pair (r_0, D) :

$$\mathcal{K}_k = \text{span}\{r_0, Dr_0, \dots, D^{k-1}r_0\} ,$$

where $1 \leq k \leq m$, with m being the rank of D . The simplest example consists of the pair r_0 and the identity matrix I , in which case $k = 1$ and the Krylov subspace is simply the vector r_0 . In this case we have to do with an *invariant subspace*: further multiplications of r_0 by $D = I$ will not increase the subspace.

Iterative methods which seek solutions x in \mathcal{K}_k are called Krylov subspace methods. If $Q_k = [q_1, \dots, q_k]$ is a basis of orthonormal vectors of \mathcal{K}_k , the approximate solution can be written as

$$x_k = x_0 + \sum_{i=1}^k y_i q_i$$

In order to compute it one has to compute first $q_i, i = 1, 2, \dots, k$. There are two general approaches to compute y , namely

- i) Galerkin approach: choose y such that the residual vector r_k is orthogonal to \mathcal{K}_k .
- ii) Minimal residual approach: choose y such that $\|r_k\|$ is minimal.

Basis generation: Arnoldi Algorithm

The method is a modified Gram-Schmidt orthogonalisation of \mathcal{K}_k , in which the next vector is computed by

$$\tilde{q}_{k+1} = Dq_k - \sum_{j=1}^k q_j h_{jk} ,$$

and where the coefficients h_{jk} are chosen such that the vectors come mutually orthonormal:

$$q_j^* \tilde{q}_{k+1} = 0 .$$

From this condition we get

$$h_{jk} = q_j^* Dq_k .$$

The algorithm that facilitates this process is called *Arnoldi algorithm* [7]. Having basis vectors one can construct two linear solvers, which are described in the following.

Algorithm 1 Arnoldi algorithm

```
 $\rho = \|r_0\|$   
 $q_1 = r_0/\rho$   
for  $k = 1, \dots$  do  
   $w = Dq_k$   
  for  $j = 1, \dots, k$  do  
     $h_{kj} = q_j^* w$   
     $w := w - q_j h_{jk}$   
  end for  
   $h_{k+1,k} = \|w\|$   
  if  $h_{k+1,k} = 0$  then  
    stop  
  end if  
   $q_{k+1} = w/h_{k+1,k}$   
end for
```

FOM: Full Orthogonalisation Method

If we denote H_k the matrix with elements h_{ij} , $i, j = 1, \dots, k$, the result of Arnoldi decomposition can be written in matrix form:

$$DQ_k = Q_k H_k + h_{k+1,k} q_{k+1} e_k^T \equiv Q_{k+1} \tilde{H}_k .$$

Approximate solution can also be written as

$$x_k = x_0 + Q_k y_k .$$

For the residual error vector one can write:

$$\begin{aligned} r_k &= b - Dx_k \\ &= r_0 - DQ_k y_k \\ &= q_1 \rho - Q_k H_k y_k - h_{k+1,k} q_{k+1} e_k^T y_k . \end{aligned}$$

The Galerkin approach requires the next residual to be orthonormal to all previous vectors

$$Q_k^* r_k = 0 ,$$

which is

$$Q_k^* q_1 \rho - Q_k^* Q_k H_k y_k - Q_k^* q_{k+1} h_{k+1,k} e_k^T y_k = 0 .$$

Using orthonormality of Q_k ,

$$\begin{aligned} Q_k^* q_1 &= e_1 , \\ Q_k^* Q_k &= I_k , \\ Q_k^* q_{k+1} &= 0 , \end{aligned}$$

one obtains the linear system

$$H_k y_k = e_1 \rho .$$

Note that H_k is an upper Hessenberg matrix and that the size of the problem depends on the value of k , which is usually a much smaller than N , the order of the original problem.

GMRES: Generalised Minimal Residual Method

Arnoldi recurrences can be written also in the form:

$$DQ_k = Q_k H_k + h_{k+1,k} q_{k+1} e_k^T \equiv Q_{k+1} \tilde{H}_k ,$$

where now \tilde{H}_k is an upper Hessenberg $(k+1) \times k$ matrix, or the matrix H_k appended by the row $h_{k+1,k} e_k^T$. With this notations the residual error vector can be written as

$$r_k = q_1 \rho - Q_{k+1} \tilde{H}_k y_k .$$

The minimal residual strategy of GMRES [8] requires that

$$\|b - Dx_k\| \rightarrow \min, \quad x_k \in \mathcal{K}_k .$$

Substituting $x_k = Q_k y_k$ and $q_1 = Q_{k+1} e_1$ we get

$$\left\| Q_{k+1} (e_1 \rho - \tilde{H}_k y_k) \right\| \rightarrow \min .$$

Since Q_{k+1} is orthonormal, it can be ignored and we get the smaller least squares problem:

$$\left\| e_1 \rho - \tilde{H}_k y_k \right\| \rightarrow \min, \quad y_k \in \mathbb{C}^k .$$

Krylov solvers are Polynomial Approximation solvers

In fact, the approximate solution in the Krylov subspace

$$x_k \in \mathcal{K}_k = \text{span}\{r_0, Dr_0, \dots, D^{k-1}r_0\} ,$$

can be described as a degree $k - 1$ polynomial applied to r_0 :

$$x_k = x_0 + P_{k-1}(D)r_0 .$$

Then, the residual vector is a degree k polynomial applied to r_0 :

$$\begin{aligned} r_k &= r_0 - DP_{k-1}(D)r_0 \\ &= [I - DP_{k-1}(D)] r_0 \\ &\equiv R_k(D)r_0 . \end{aligned}$$

Hence, GMRES solves the constrained minimisation problem: find the polynomial R_k such that

$$\|R_k(D)r_0\| \rightarrow \min , \quad R_k(0) = 1 .$$

In fact, this is a characterisation of Krylov subspace methods. One speaks of *optimal polynomials* generated in this way.

But ...

... GMRES requires to store all Arnoldi vectors and its work grows proportionally to k^2 . One can limit this growth of resources by restarting the algorithm after a given number of steps. Using this strategy, robustness is lost and sometimes convergence as well. Going back to normal equations,

$$D^* D x = D^* b ,$$

we know that the optimal polynomial is computed for $D^* D$ and *not* for D itself. However, computing resources remain constant in this case, an important advantage over GMRES. Therefore, a great deal of research has been devoted to methods which are as cheap as CGNE and yet have similar convergence to GMRES.

BiCG γ_5

One of these methods is the specialisation of the Biconjugate Gradients (BiCG) algorithm in the case of the Wilson operator, which is γ_5 -Hermitian (see [5] p47):

$$D^* = \gamma_5 D \gamma_5 .$$

The method, coined BiCG γ_5 , can be formally obtained from CG by inserting a γ_5 operator whenever a scalar product occurs:

$$u^* v \longrightarrow u^* \gamma_5 v .$$

Since, γ_5 is a nondefinite operator, this scalar product may not exist, and a premature breakdown may occur. In practice we see an irregular behaviour of the residual vector norm history.

BiCGStab

Biconjugate Gradients Stabilised algorithm, or BiCGStab [9] replaces the redundant recursion of BiCG for a local minimiser of the residual vector norm, thus giving a general and robust solver for non-Hermitian systems.

4 QCDLAB 1.0

QCDLAB is designed to be a high level language interface for lattice QCD computational procedures. It is based on the MATLAB and OCTAVE language and environment. While MATLAB is a product of The MathWorks, OCTAVE is its clone, a free software under the terms of the GNU General Public License.

MATLAB/OCTAVE is a technical computing environment integrating numerical computation and graphics in one place, where problems and solutions look very similar and sometimes almost the same as they are written mathematically. Main features of MATLAB/OCTAVE are:

- Vast Build-in mathematical and linear algebra functions.
- Many functions form Blas, Lapack, Minpack, etc. libraries.
- State-of-the-art algorithms.
- Interpreted language.
- Dynamically loaded modules from other languages like C/C++, FORTRAN.
- Ability to compile OCTAVE codes using the Startego Octave Compiler, `Octave-Compiler.org`.

Hence, QCDLAB offers a two level language system: a higher level language, which is very popular for numerical work and a lower level translation to C++. In fact, if required the lower level can be further optimised for the particular hardware in place.

The first version of QCDLAB is intended for work on the higher level only. QCDLAB 1.0 contains the following MATLAB/OCTAVE functions:

Autocorel	BiCGg5	BiCGstab	Binning	cdot5
CG	CGNE	Dirac_KS	Dirac_r	Dirac_W
FOM	Force_KS	Force_W	GMRES	HMC_KS
HMC_W	Lanczos	SCG	SUMR	wloop

We divide them in two groups: simulation and inversion algorithms. We begin below with the description of simulation algorithms.

4.1 Simulation Algorithms

This section introduces QCDLAB 1.0 simulation tools of lattice QED2. In this case, lattice gauge fields $U_{\mu,i}$ can be expressed using angles $\theta_{\mu,i} \in \mathbb{R}$,

$$U_{\mu,i} = e^{i\theta_{\mu,i}} ,$$

whereas gauge action is given by

$$S_g = \beta \sum_{i,\mu < \nu} [1 - \cos(\theta_{\mu,i} + \theta_{\nu,i+\hat{\mu}} - \theta_{\mu,i+\hat{\nu}} - \theta_{\nu,i})] ,$$

where $\beta = 1/e^2$, and electron charge e .

Dirac Operators

In case of Wilson fermions the Dirac operator is given by

$$D_{ij} = (m + \frac{4}{a})I_2 \delta_{ij} - \frac{1}{2} \sum_{\mu=1}^2 [(I_2 - \sigma_{\mu})U_{\mu,i}\delta_{i,j+\hat{\mu}} + (I_2 + \sigma_{\mu})U_{\mu,i-\hat{\mu}}\delta_{i,j-\hat{\mu}}] ,$$

with σ_{μ} being Pauli matrices,

$$\sigma_1 = \begin{pmatrix} 0 & 1 \\ 1 & 0 \end{pmatrix}, \quad \sigma_2 = \begin{pmatrix} 0 & -i \\ i & 0 \end{pmatrix}, \quad \sigma_3 = \begin{pmatrix} 1 & 0 \\ 0 & -1 \end{pmatrix} .$$

QCDLAB defines spin projection operators in terms of these matrices

$$\mathcal{P}_{\mu}^{+} = \frac{1}{2}(I_2 + \sigma_{\mu}), \quad \mathcal{P}_{\mu}^{-} = \frac{1}{2}(I_2 - \sigma_{\mu}) .$$

They are computed using this code:

% Form spin projection operators

```
P1_plus = [1,1;1,1]/2; P1_minus = [1,-1;-1,1]/2;
P2_plus = [1,-i;i,1]/2; P2_minus = [1,i;-i,1]/2;
```

Given the quark mass, `mass`, the number of lattice sites along each direction, `N`, the total number of lattice sites, `N2`, the gauge field configuration, `U1`, and spin projector operators as input, `Dirac_W` returns Wilson matrix, `A1`:

```
A1=Dirac_W(mass,N,N2,U1,P1_plus,P2_plus,P1_minus,P2_minus);
```

For staggered fermions we have

$$D_{ij} = m \delta_{ij} + \frac{1}{2} \sum_{\mu=1}^2 \epsilon_{\mu,i} (U_{\mu,i} \delta_{i,j+\hat{\mu}} - U_{\mu,i-\hat{\mu}} \delta_{i,j-\hat{\mu}}),$$

where

$$\epsilon_{1,i} = 1, \quad \epsilon_{2,i} = (-1)^{i_1}.$$

`Dirac_KS` below returns the staggered matrix:

```
A1=Dirac_KS(mass,N,N2,U1);
```

Forces

In order to compute the force it is convenient to have ready a nearest neighbours list for each lattice site. The code that implement forward `kp` and backward `km` lists is given below.

% Make nearest neighbours list

```
for j2=0:N-1;
for j1=0:N-1;
k = 1 + j1 + j2*N;
kp(k,1) = 1 + mod(j1+1,N) + j2*N;
kp(k,2) = 1 + j1 + mod(j2+1,N)*N;
km(k,1) = 1 + mod(j1-1+N,N) + j2*N;
km(k,2) = 1 + j1 + mod(j2-1+N,N)*N;
end
end
```

In case of two degenerate Wilson fermions, the force is given by

$$F_{\mu,i} = -\beta \sin(\theta_{\mu,i} + \theta_{\nu,i+\hat{\mu}} - \theta_{\mu,i+\hat{\nu}} - \theta_{\nu,i}) + 2Re iU_{\mu,i}^* (\chi_{i+\hat{\mu}}^* \mathcal{P}_{\mu}^+ \eta_i + \eta_{i+\hat{\mu}}^* \mathcal{P}_{\mu}^- \chi_i),$$

where pseudofermion fields are two-component complex valued vectors. `Force_W` returns both gauge `pg` and fermion `pf` pieces. Its arguments are: number of lattice sites, `N2`, forward neighbour list, `kp`, backward neighbour list, `km`, angles, `theta1`, pseudofermion fields, `eta`, `chi`, gauge field, `U1`, and spin projector operators.

```
[pf,pg]=Force_W(N2,kp,km,theta1,eta,chi,U1,P1_plus,P2_plus,P1_minus,P2_minus);
```

In case of four degenerate Kogut-Susskind fermions the force is

$$F_{\mu,i} = -\beta \sin(\theta_{\mu,i} + \theta_{\nu,i+\hat{\mu}} - \theta_{\mu,i+\hat{\nu}} - \theta_{\nu,i}) + 2Re iU_{\mu,i}^* (\epsilon_{\mu,i+\hat{\mu}} \chi_{i+\hat{\mu}}^* \eta_i - \epsilon_{\mu,i} \eta_{i+\hat{\mu}}^* \chi_i),$$

where pseudofermion fields are complex values numbers. As in Wilson case, `Force_KS` returns gauge `pg` and fermion `pf` forces.

```
[pf,pg]=Force_KS(N2,kp,km,theta1,eta,chi,U1);
```

Simulation Tools

QCDLAB's simulation tools are `HMC_W` and `HMC_KS`. Their arguments are:

`iconf`: set to zero for *hot* start,

`theta1`: starting angles.

On completion they return:

A2: Dirac operator on theta2 background,
 PlaQ: plaquette history,
 Q_top: topological charge history,
 Wloop: ten smallest Wilson loops history,
 theta2: output angles,
 stat: a four column array of Metropolis test history.

One trajectory of Hybrid Monte Carlo algorithm consists of steps given in Algorithm 2. In case of a successful test, the

Algorithm 2 HMC Trajectory in QCDLAB

- Heatbath update of pseudofermion fields $\phi = A1 * \eta_0$;
 - Heatbath update of momenta $P = \text{randn}(N2, 2)$;
 - Compute Hamiltonian H1.
 - Invert Dirac operator $\chi = A1' \backslash \eta_0$;
 - Advance momenta half step $P = P + p \cdot \text{dot} * \text{deltat} / 2$;
 - Start molecular dynamics loop.
 - Advance angles full step $\text{theta2} = \text{theta2} + P * \text{deltat}$;
 - Compute inversions $\eta = A2 \backslash \phi$; $\chi = A2' \backslash \eta$;
 - Advance momenta full step $P = P + p \cdot \text{dot} * \text{deltat}$;
 - Advance angles full step $\text{theta2} = \text{theta2} + P * \text{deltat}$;
 - Compute inversions $\eta = A2 \backslash \phi$; $\chi = A2' \backslash \eta$;
 - Advance momenta half step $P = P + p \cdot \text{dot} * \text{deltat} / 2$;
 - Compute Hamiltonian H2.
 - Perform Metropolis test.
-

function computes topological charge,

$$Q_{\text{top}} = \frac{1}{2\pi} \sum_{i, \mu < \nu} \sin(\theta_{\mu, i} + \theta_{\nu, i + \hat{\mu}} - \theta_{\mu, i + \hat{\nu}} - \theta_{\nu, i}),$$

and $n \times n$ Wilson loops,

$$W_n = \frac{1}{N} \sum_{i, \mu < \nu} \cos \left(\sum_{k=0}^{n-1} \theta_{\mu, i + k\hat{\mu}} + \sum_{k=0}^{n-1} \theta_{\nu, i + n\hat{\mu} + k\hat{\nu}} - \sum_{k=0}^{n-1} \theta_{\mu, i + n\hat{\nu} + k\hat{\mu}} - \sum_{k=0}^{n-1} \theta_{\nu, i + k\hat{\nu}} \right).$$

HMC_W and HMC_KS functions are called in the form given below.

```
[A2, PlaQ, Q_top, Wloop, theta2, stat] = HMC_W(theta1, iconf);
[A2, PlaQ, Q_top, Wloop, theta2, stat] = HMC_KS(theta1, iconf);
```

Computation of Wilson Loops

wloop returns ten smallest Wilson loops. Angles $\theta_{\mu, i}, \theta_{\mu, i + \hat{\mu}}, \dots, \theta_{\mu, i + 9\hat{\mu}}$ are implemented using arrays tleg1, tleg2...tlog10. These are summed over to give arrays wleg1, wleg2...wlog10. Then, each of these arrays is used to compute the corresponding Wilson loop around a square. The function is called using:

```
wlp = wloop(N, N2, kp, km, theta1);
```

Autocorrelations and Errors

When measuring an observable, such as plaquette, we get time series of data in the form $\mathcal{O}_i, i = 1, 2, \dots, n$. Standard error estimation procedures rely on the assumption that data are *decorrelated*. This can be checked by measuring the autocorrelation function

$$A(t) = \text{cov}(\mathcal{O}(0)\mathcal{O}(t)) \sim e^{-t/t_{\text{exp}}},$$

where t_{exp} is called *exponential autocorrelation time*. `Autocorel`, which implements $A(t)$, has two arguments: the data vector, `x`, and the maximal time interval, `t`:

```
y=Autocorel(x,t);
```

In fact, a quick way to estimate the error is to block or ‘bin’ data. In this case one computes block averages and estimates the error of averages for increasing block size. `Binning` does exactly that. One must specify the original data, `x`, and the maximal block size, `t`. It returns a t -element vector `err`, containing error estimates for block sizes $1, 2, \dots, t$:

```
err=Binning(x,t);
```

A simple recipe is to take $t \sim t_{\text{exp}}$ and choose the maximum value of `err`.

Computing Projects

The best way to test QCDLAB capabilities is to set up a simple computing project like the following: *Compute square Wilson loops and topological charge using HMC_KS. Graph Wilson loops as a function of the linear size. Do you get a perimeter law? Plot the histogram of the topological charge. How is it distributed?*

As usual, one opens two windows, one running MATLAB/OCTAVE, and one text editor where `HMC_KS.m` file is located. We present here an example of running OCTAVE with model and algorithmic parameters as in the listing. Entering

```
[A2, Plaq, Q_top, Wloop, theta2, stat]=HMC_KS([],0);
```

one gets an output stream that looks something like:

```
ans =
  3.00000    0.33333    0.57985   -1.25858
ans =
 16.00000    0.12500    0.76736   -0.92516
ans =
 20.00000    0.15000    0.75921   -0.27965
```

We have displayed here only the first three lines. Columns of the stream display trajectory number, acceptance, plaquette and topological charge. One can store the angle output, `theta2`, and feed it into the next run:

```
theta1=theta2;
[A2, Plaq, Q_top, Wloop, theta2, stat]=HMC_KS(theta1,1);
```

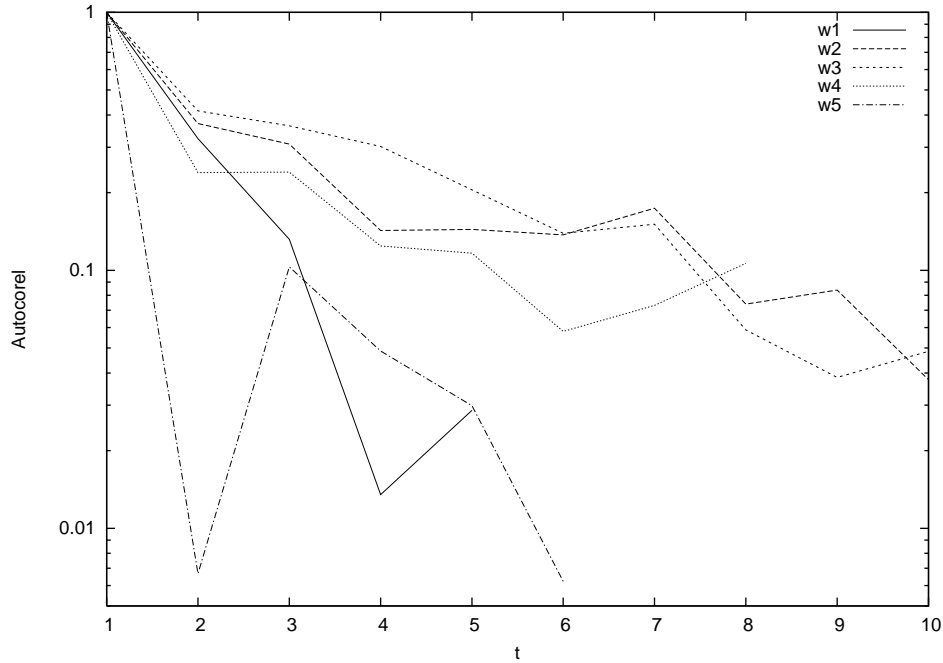
In our example project we ran seven batches of `HMC_KS` and analysed results of the last batch. We computed and plotted autocorrelation functions of five Wilson loops:

```
auto=Autocorel(Wloop(:,1),20);
semilogy(auto)
hold
auto=Autocorel(Wloop(:,2),20);
semilogy(auto)
auto=Autocorel(Wloop(:,3),20);
semilogy(auto)
auto=Autocorel(Wloop(:,4),20);
semilogy(auto)
auto=Autocorel(Wloop(:,5),20);
semilogy(auto)
xlabel('t')
ylabel('Autocorel')
replot
gset terminal postscript
gset out 'Auto.ps'
```

```

replot
gset terminal x11
hold

```



Then we computed central values of Wilson loops:

```
w=mean(Wloop);
```

The errors are estimated using Binning with the largest block size set to 10:

```

sw=max(Binning(Wloop(:,1),10));
sw=[sw,max(Binning(Wloop(:,2),10))];
sw=[sw,max(Binning(Wloop(:,3),10))];
sw=[sw,max(Binning(Wloop(:,4),10))];
sw=[sw,max(Binning(Wloop(:,5),10))];
sw=[sw,max(Binning(Wloop(:,6),10))];
sw=[sw,max(Binning(Wloop(:,7),10))];
sw=[sw,max(Binning(Wloop(:,8),10))];
sw=[sw,max(Binning(Wloop(:,9),10))];
sw=[sw,max(Binning(Wloop(:,10),10))];

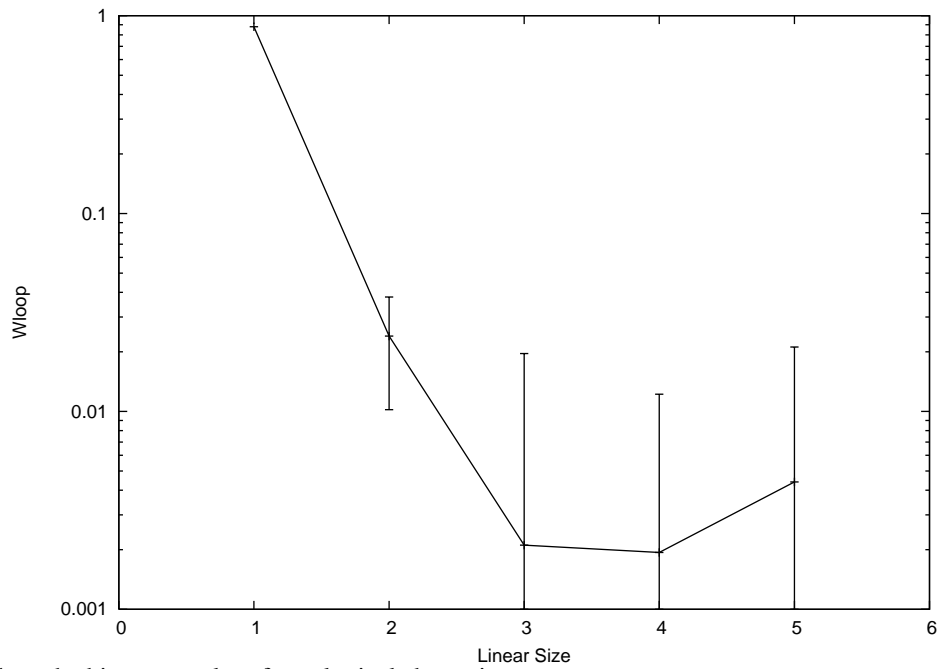
```

Then, to plot Wilson loops we entered:

```

semilogyerr(w(1:5),sw(1:5))
hold
axis([0,6,1e-4,1])
semilogy(w(1:5))
axis([0,6,1e-3,1])
xlabel('Linear Size')
ylabel('Wloop')
replot
gset terminal postscript
gset out 'Wloop.ps'
replot
gset terminal x11
hold

```

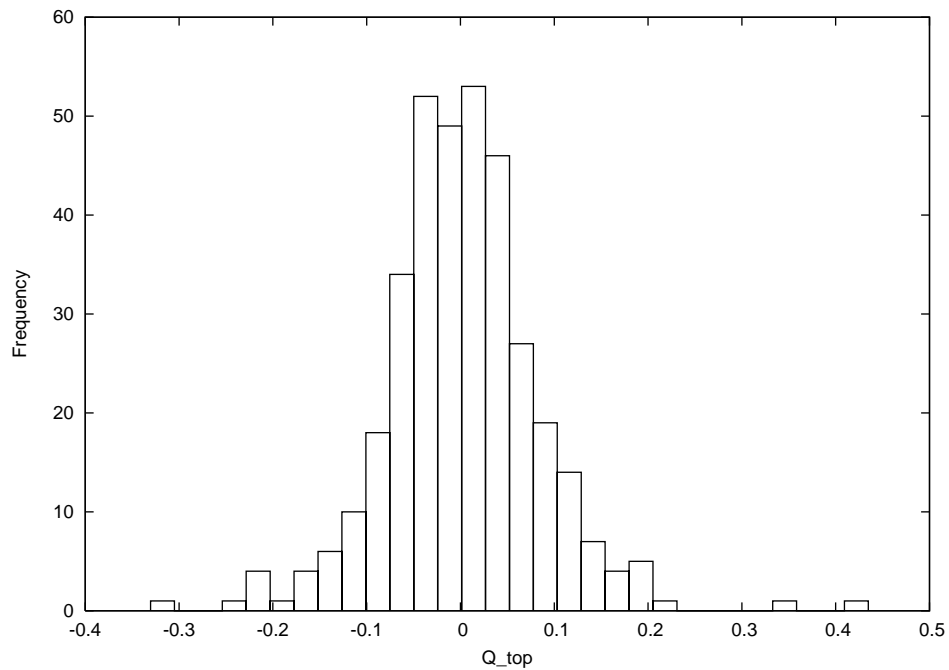


Finally, to produce the histogram plot of topological charge is very easy:

```

hist(Q_top,30)
xlabel('Q_top')
ylabel('Frequency')
gset terminal postscript
gset out 'Q_top.ps'
replot
gset terminal x11
hold

```



4.2 Inversion Algorithms

In this section we list QCDLAB functions which implement basic Krylov subspace inverters for use in lattice gauge theories. In this version the whole matrix A , be it sparse or dense, should be supplied as an argument, together with the right hand side b , the approximate solution x_0 , the tolerance tol and the maximum number of iterations $nmax$. `CG.m` and `CGNE.m` functions below return solution x and *recursive* residual vector norm history rr .

```
[x, rr] = CG(A, b, x0, tol, nmax);
[x, rr] = CGNE(A, b, x0, tol, nmax);
```

`FOM.m` and `GMRES.m` return *true* residual instead of recursive residual and Arnoldi matrix H as well. This can be used to compute approximate eigenvalues of the original matrix A .

```
[z, rt, H] = FOM(A, b, z0, tol, nmax);
[z, rt, H] = GMRES(A, b, z0, tol, nmax);
```

BiCG γ_5 and BiCGstab

The `BiCGg5` function may be used for γ_5 -Hermitian operators:

```
[x, rr] = BiCGg5(A, b, x0, tol, nmax);
```

It uses a special inner product, a pseudo-scalar which does not lead to a vector norm. Hence, the algorithm can break down prematurely. There are *look ahead* strategies which cure this problem. We don't employ them. However, to avoid a starting breakdown the recipe is to use a non-trivial initial solution.

`BiCGstab` is a general non-Hermitian solver. It inherits from `BiCG` the premature breakdown problem. In order to avoid a starting breakdown we use a random initial *left Lanczos vector* y_0 .

```
[z, rr]=BiCGstab(A, b, z0, tol, nmax);
```

Symmetric Lanczos algorithm

The counterpart of Arnoldi algorithm for Hermitian matrices is Lanczos algorithm [10]. From Arnoldi algorithm we have

$$H_k = Q_k^* A Q_k .$$

If A is Hermitian we can write

$$H_k^* = Q_k^* A^* Q_k = Q_k^* A Q_k = H_k .$$

Since H_k is upper Hessenberg and Hermitian, it must be tridiagonal. It is commonly denoted by T_k . This way, after k Lanczos steps we have

$$A Q_k = Q_k T_k + \beta_k q_{k+1} e_k^T ,$$

where

$$T_k = \begin{pmatrix} \alpha_1 & \beta_1 & & & \\ \beta_1 & \alpha_2 & \ddots & & \\ & \ddots & \ddots & \beta_{k-1} & \\ & & & \beta_{k-1} & \alpha_k \end{pmatrix}$$

QCDLAB function `Lanczos` arguments are matrix A , starting vector b and maximal number of steps $nmax$. It returns Lanczos vectors Q and matrix T :

```
[Q, T]=Lanczos(A, b, nmax);
```

Computing Projects

In this section we illustrate QCDLAB inverter functions for Wilson fermions. The matrix A , a function argument, is an output of `HMC_W`. Having an angle configuration, one can generate it using `Dirac_r` function: given the quark mass $mass$, the Wilson parameter r , the lattice size N , the total number of lattice sites $N2$, and the angle configuration $theta1$ as arguments, it returns the Wilson-Dirac matrix $A1$:

```
A1=Dirac_r(mass, r, N, N2, theta1);
```

Note that knowing A is not essential. Indeed, any user supplied procedure of matrix-vector multiplication can be called whenever `=A*` occurs in the function. Future releases of QCDLAB will provide capabilities that implement this.

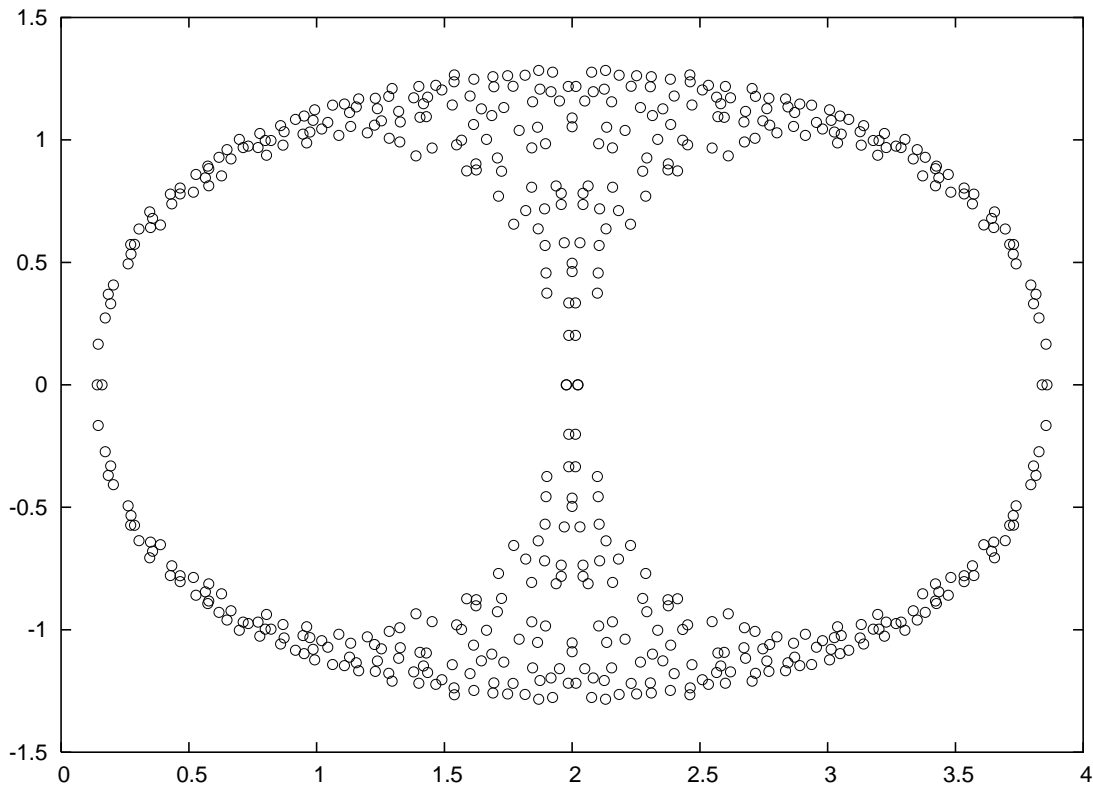
Wilson Fermions

In our example project here, we used an angle configuration on a 16×16 lattice. We loaded this configuration and created a right hand side and a starting solution. Then we generated three Wilson-Dirac matrices of three different fermion masses:

```
load theta16
N=16;N2=N^2;b=zeros(2*N2,1);x0=b;b(1)=1;
A1=Dirac_r(-0.1,1,N,N2,theta2);
A2=Dirac_r(-0.05,1,N,N2,theta2);
A3=Dirac_r(0,1,N,N2,theta2);
```

A first thing to do is to compute and plot eigenvalues of the massless operator:

```
e3=eig(A3);
plot(e3,'o')
```



In order to compare GMRES and CGNE convergence one calls respective solvers for each fermion mass as follows:

```
tol=1e-13;nmax=2*N2;
[x_gmres1,r_gmres1,H1] = GMRES(A1,b,x0,tol,nmax);
[x_gmres2,r_gmres2,H2] = GMRES(A2,b,x0,tol,nmax);
[x_gmres3,r_gmres3,H3] = GMRES(A3,b,x0,tol,nmax);
[x_cgne1,r_cgne1] = CGNE(A1,b,x0,tol,nmax);
[x_cgne2,r_cgne2] = CGNE(A2,b,x0,tol,nmax);
[x_cgne3,r_cgne3] = CGNE(A3,b,x0,tol,nmax);
```

Then one plots the residual norm history as a function of matrix-vector multiplications calls:

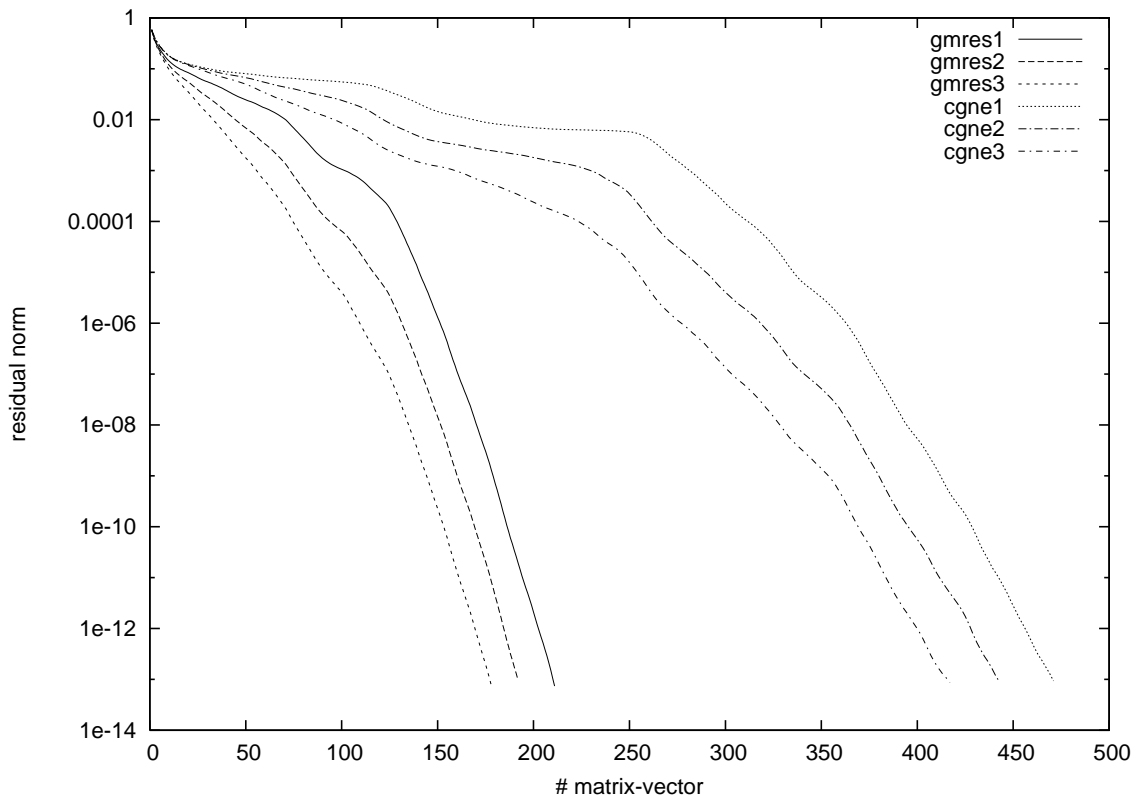
```
k_gmres1=max(size(r_gmres1));
k_gmres2=max(size(r_gmres2));
k_gmres3=max(size(r_gmres3));
k_cgne1=2*max(size(r_cgne1));
k_cgne2=2*max(size(r_cgne2));
k_cgne3=2*max(size(r_cgne3));
semilogy(1:k_gmres1,r_gmres1,'gmres1;')
```

```

hold
semilogy(1:k_gmres2,r_gmres2,';gmres2;')
semilogy(1:k_gmres3,r_gmres3,';gmres3;')
semilogy(1:2:k_cgne1,r_cgne1,';cgne1;')
semilogy(1:2:k_cgne2,r_cgne2,';cgne2;')
semilogy(1:2:k_cgne3,r_cgne3,';cgne3;')
xlabel('#\u2264matrix-vector')
ylabel('residual\u2264norm')
replot
gset terminal postscript
gset out 'conv_hist.ps'
replot
gset terminal x11
hold

```

Note that GMRES has an additional overhead which grows like i^2 , rendering the algorithm useless for large i . Hence, the GMRES convergence, measured in terms of matrix-multiplication number, should be considered as a theoretically ideal result and a benchmark for the performance of short-recurrences algorithms.



The difficulty of GMRES exploding resources can be avoided using BiCGg5 and BiCGstab functions. Employing the lightest mass one can compare convergence history of all solvers:

```

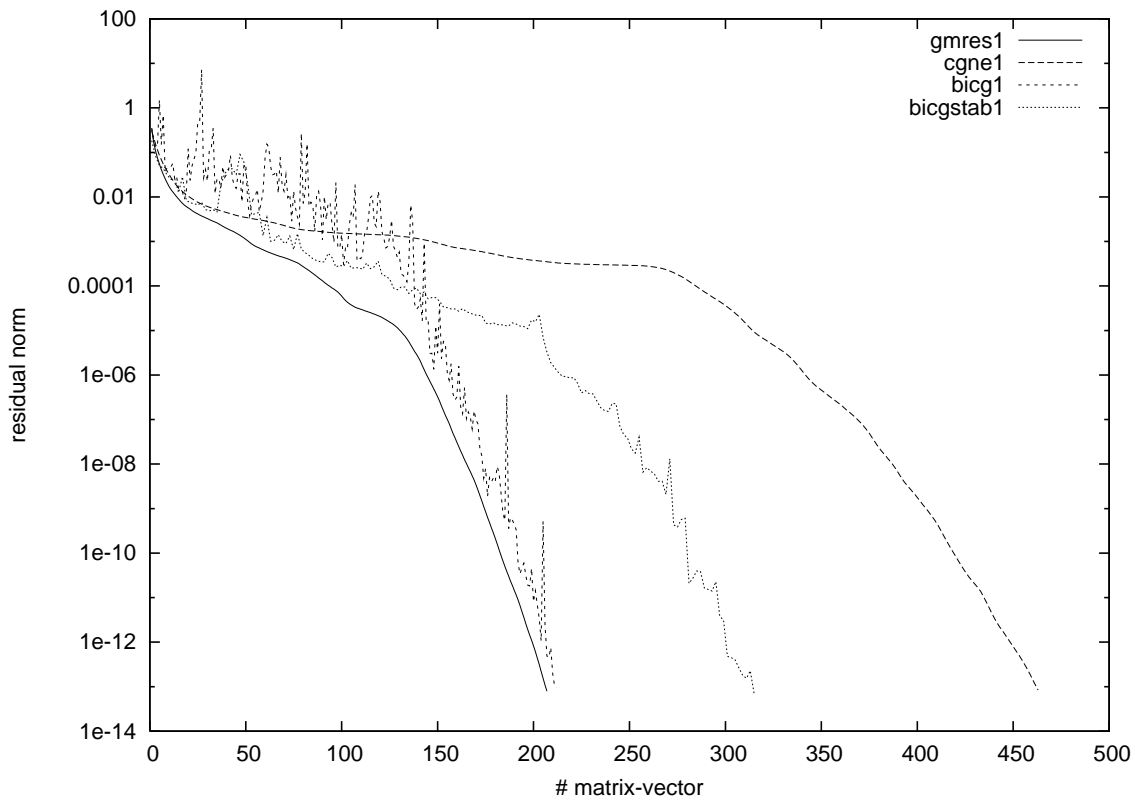
x0=rand(2*N2,1);
[x_gmres1,r_gmres1,H1] = GMRES(A1,b,x0,tol,nmax);
[x_cgne1,r_cgne1] = CGNE(A1,b,x0,tol,nmax);
[x_bicg1,r_bicg1] = BiCGg5(A1,b,x0,tol,nmax);
[x_bicgstab1,r_bicgstab1]=BiCGstab(A1,b,x0,tol,nmax);
k_gmres1=max(size(r_gmres1));
k_cgne1=2*max(size(r_cgne1));
k_bicg1=max(size(r_bicg1));
k_bicgstab1=2*max(size(r_bicgstab1));
semilogy(1:k_gmres1,r_gmres1,';gmres1;')
hold

```

```

semilogy (1:2:k_cgne1 , r_cgne1 , ' ; cgne1 ; ' )
semilogy (1:k_bicg1 , r_bicg1 , ' ; bicg1 ; ' )
semilogy (1:2:k_bicgstabl , r_bicgstabl , ' ; bicgstabl ; ' )
xlabel ( '#_matrix-vector' )
ylabel ( 'residual_norm' )
replot
gset terminal postscript
gset out 'all_solver_conv_hist.ps'
replot
gset terminal x11
hold

```



As seen from the plot, the best short-recurrences solver (for this particular example) is BiCGg5. It converges at about the same matrix-vector multiplications as GMRES and yet avoiding its pitfalls. Its irregular convergence history can be softened to the level of BiCGstab using the *quasiminimal residual approach*, or QMR algorithm, which is not described here.

Staggered Fermions

Staggered operator is anti-Hermitian as can be illustrated below: first create the staggered matrix; then typing `norm(A+A')`, the answer will be zero. Since $i * A$ is Hermitian, its eigenvalues will be real. We plotted the eigenvalues as sorted from the `eig` function.

```

U1=cos ( theta2 )+sqrt (-1)*sin ( theta2 );
N=16;N2=N^2;
A=Dirac_KS (0,N,N2,U1);
norm(A+A')
ea=eig ( i *A );
plot ( ea , 'o' ; ea ; ' )

```

Theory tells that for normal matrices, such as staggered operator, CGNE is an optimal solver. The following plot compares GMRES and CGNE convergence history as a function of matrix-vector multiplications counter.

```

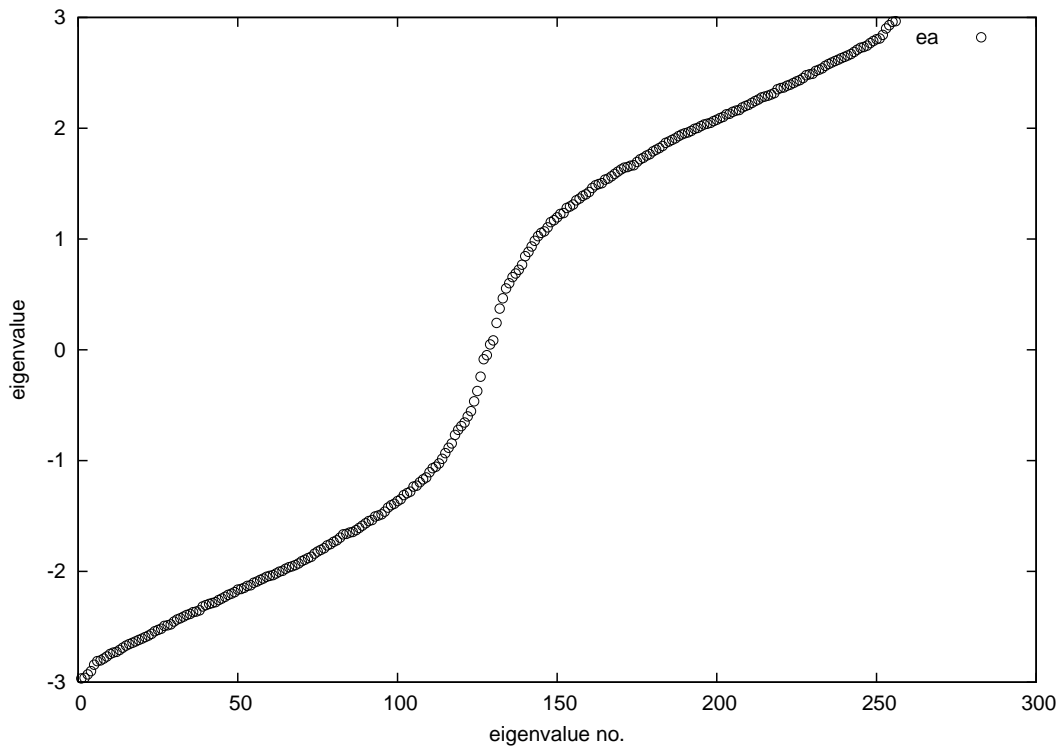
b=zeros (N2,1); x0=b; b(1)=1;

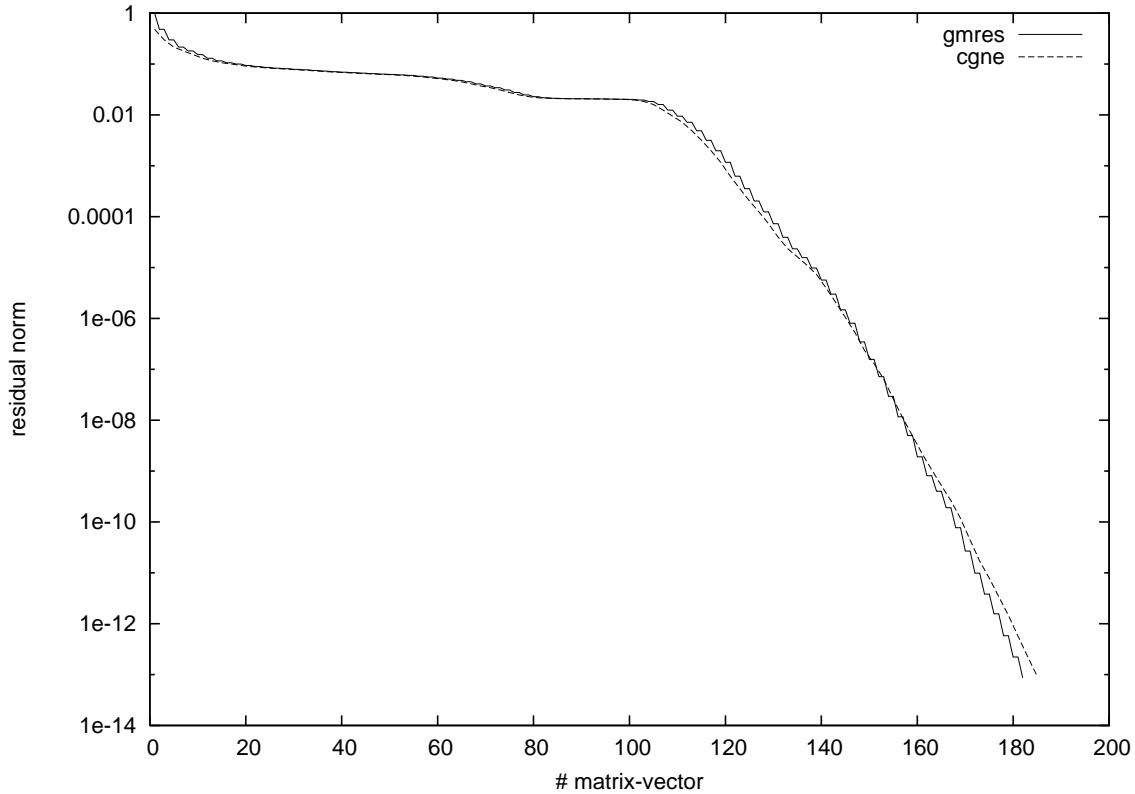
```

```

tol=1e-13;nmax=N2;
[x_gmres , r_gmres , H] = GMRES(A,b,x0 , tol , nmax);
[x_cgne , r_cgne ] = CGNE(A,b,x0 , tol , nmax);
k_cgne=max( size( r_cgne ) );
semilogy( r_gmres , ' ; gmres ; ' )
hold
semilogy( 1:2:2*k_cgne , r_cgne , ' ; cgne ; ' )
xlabel( '#_matrix-vector' )
ylabel( 'residual_norm' )
replot
gset terminal postscript
gset out 'conv_hist_ks.ps'
replot
gset terminal x11
hold

```





CG-Lanczos Equivalence

As another application, one can use Lanczos algorithm to solve the linear system

$$D^* D x = D^* b$$

for Wilson matrix D . Taking the lightest mass from the previous example and setting maximal iteration number to `k_cgne3`:

```
[Q,T]=Lanczos(A3'*A3,A3'*b,k_cgne3);
```

one can construct the solution using:

```
x_lanczos3=Q(:,1:k_cgne3)*(T\([norm(A3'*b); zeros(k_cgne3-1,1)]));
```

Comparison to `x_cgne3` yields:

```
norm(x_cgne3-x_lanczos3)
ans = 2.5537e-14
```

This example illustrates the theoretical result that CG and Lanczos algorithms are equivalent linear solvers in exact arithmetic.

4.3 Ginsparg-Wilson Fermions

In this section we describe QCDLAB functions for use with lattice chiral fermions. A chiral lattice Dirac operator satisfies the Ginsparg-Wilson relation [11]:

$$\gamma_5 D + D \gamma_5 = 2 D \gamma_5 D .$$

One solution to this relation is the Nueberger overlap operator [12],

$$D = \frac{1+m}{2} I + \frac{1-m}{2} \gamma_5 \text{sgn}(H_W) ,$$

where $\text{sgn}(\cdot)$ is the signum function, $H_W = \gamma_5 D_W$. For the signum function to be nontrivial, the Wilson-Dirac operator should be indefinite, which is the case if its bare mass M is sufficiently negative. This is usually taken to be in the interval $(-2, 0)$.

Another form of the Neuberger operator is

$$D = \frac{1+m}{2} I + \frac{1-m}{2} D_W (D_W^* D_W)^{-\frac{1}{2}} .$$

If we express D_W in terms of its singular values and vectors,

$$D_W = U \Sigma V^* ,$$

we get

$$D = \frac{1+m}{2} I + \frac{1-m}{2} UV^* ,$$

Since U and V are unitary operators, so it is UV^* . Hence, the overlap operator is a shifted unitary operator. Iterative inverters for such operators can be simplified as we show below. Before doing this we give an iterative method in order to compute the overlap operator.

Lanczos Algorithm for the Overlap Computation

In order to apply the overlap operator to a vector b one should first perform the inversion $(D_W^* D_W)^{1/2} x = b$ and then apply D_W to x . The calculation is based on the following integral representation for the inverse square root [13]:

$$(D_W^* D_W)^{-1/2} = \frac{2}{\pi} \int_0^\infty dt (t^2 + D_W^* D_W)^{-1} .$$

From the previous section we know that one can use the Lanczos algorithm to solve the linear systems, such as

$$(D_W^* D_W)^{-1} b = Q_k T_k^{-1} e_1 \rho , \quad (4.1)$$

where $\rho = \|b\|$. Since by shifting the matrix $D_W^* D_W$ one obtains the same Lanczos vectors, we can write

$$(t^2 + D_W^* D_W)^{-1} b = Q_k (t^2 + T_k)^{-1} e_1 \rho . \quad (4.2)$$

Using the above integral representation again, but now for Lanczos matrix T_k we get

$$x = (D_W^* D_W)^{-1/2} b = Q_k T_k^{-1/2} e_1 \rho . \quad (4.3)$$

To summarise, in order to find x one computes:

- Q_k and T_k using the Lanczos function on $D_W^* D_W$ and b ,
- then computes $y_k = T_k^{-1/2} e_1 \rho$,
- and finally $x = Q_k y_k$.

Using the `A3`, `b` pair of the last example one can enter these commands:

```

b=rand(2*N2,1);
rho=norm(b);
[Q,T]=Lanczos((A3-eye(512))'*(A3-eye(512)),b,200);
[N,k]=size(Q);
e1=zeros(k-1,1); e1(1)=1;
y=sqrtm(T)\e1*rho;
x=(A3-eye(512))*Q(:,1:k-1)*y;

```

In case Q_k vectors are too large to be stored in the main memory of the computer, one can modify `Lanczos` such that it does not accumulate Lanczos vectors into `Q`. In this case, one calculates y_k and then repeats the Lanczos iteration in order to form x . This is the so called *double pass algorithm*.

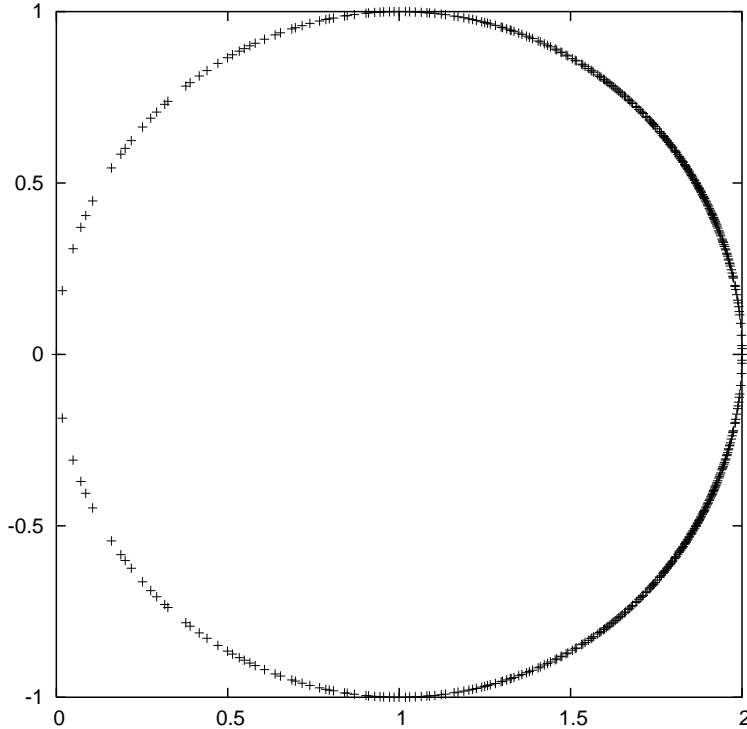
For small problems, as it is usually the case for QED2 on the lattice, one can compute the overlap operator using the singular value decomposition:

```

[U_W, S_W, V_W]=svd(A3-eye(512));
V=U_W*V_W';
z=V*b;
norm(z-x)
D=eye(512)+V;
eigD=eig(D);
plot(eigD, '+')

```

In this case it is easy to compute D eigenvalues using direct methods, such as `eig` function. The following plot shows the eigenvalues of the massless overlap operator D .



Inversion of the Overlap Operator

Having computed D the next step is its inversion. Before discussing this, we note that D^*D is optimally inverted using the GGNE algorithm, the reason being the normality of D , i.e. $D^*D = DD^*$. Hence, for dynamical fermion simulations, which require D^*D inversions, CGNE is the preferred method. For propagator calculations the situation is less clear. This has to do with differing spectral properties of D^*D and D .

SUMR Algorithm

We know that GMRES is the optimal method for non-Hermitian operators. We know also that GMRES requires very often prohibitive computer resources. However, for unitary matrices one can do better. Exploiting this fact, one can construct the SUMR or the Shifted Unitary Minimal Residual algorithm [14], which is characterised by short-recurrences and at the same time benefit from the optimal properties of GMRES:

```
[rr, x] = SUMR(b, V, rho, zeta, tol, imax);
```

Semiconjugate Gradients Algorithm

We know that the FOM is the counterpart of GMRES for the Galerkin approach to linear system solvers. Likewise one can construct the counterpart of SUMR for shifted unitary systems. This can be done using a new Arnoldi process for unitary matrices, the Arnoldi Unitary Process. In the coupled recurrences variant, the search directions of the algorithm are *semiconjugate*. Therefore, the algorithm is called the Semiconjugate Gradients (SCG) algorithm [15]:

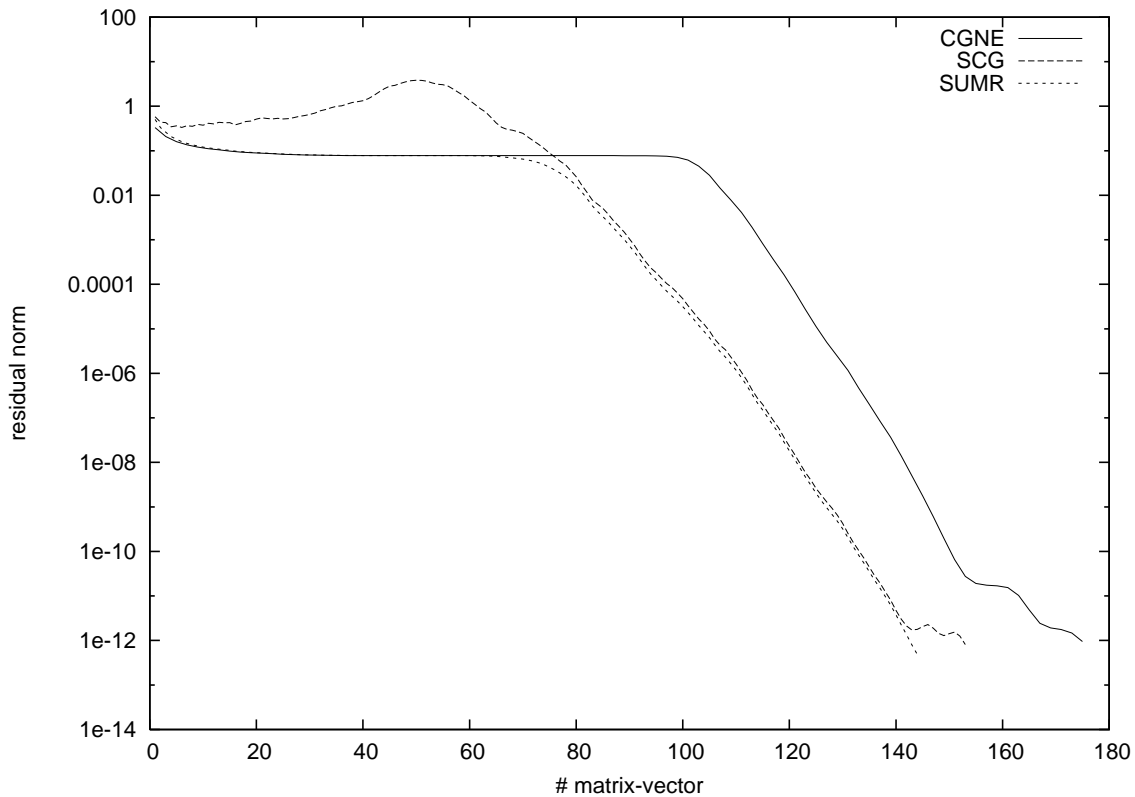
```
[x, rr] = SCG(A, b, x0, tol, nmax);
```

Computing Projects

In this section we compare CGNE, SUMR and SCG algorithms in the same background U(1) gauge field as before and the same Wilson-Dirac matrix A3:

```
m=0.0001;
D=(1+m)/2*eye(512)+(1-m)/2*V;
b=zeros(512,1);b(1)=1;
[x,rr]=CGNE(D,b,zeros(512,1),1e-12,200);
semilogy(1:2:2*max(size(rr)),rr,'-;CGNE;')
hold
[x,rr]=SCG(D,b,zeros(512,1),1e-12,200);
semilogy(rr,'-.;SCG;')
[rr,x]=SUMR(b,V,(1+m)/2,(1-m)/2,1e-12,200);
semilogy(rr,':;SUMR;')
xlabel("# matrix-vector")
ylabel("residual norm")
replot
gset terminal postscript
gset out "gw_conv_hist.ps"
replot
gset terminal x11
hold
```

The result of this comparison is shown in the following figure. One observes the optimal properties of SUMR, as expected. We note that SCG is doing worse at the beginning until it reaches the asymptotic regime of SUMR. Both SUMR and SCG are 25% faster than CGNE.



5 QCDLAB 2.x

In the previous sections we described version 1.0 of QCDLAB. Its simulation functionality is limited to the QED2 on the lattice, a very good laboratory for algorithmic and ideas exploration in lattice QCD.

We plan to extend functionality of QCDCALAB 1.0 further. We are in the designing phase of QCDCALAB 2.0 which will be totally devoted to lattice QCD simulation. The gross features of this future version are expected to be:

- Dynamically linked functions to already existing procedures in other languages.
- Ability to compile MATLAB/OCTAVE codes using the Startego Octave Compiler, `Octave-Compiler.org`.
- Scalability on various computing platforms using the above compiler.
- Extended functionality, in particular simulation functions for lattice QCD and matrix-vector multiplication procedures for various fermion operators.

References

- [1] K. G. Wilson, in *New phenomena in subnuclear Physics*, ed. A. Zichichi (Plenum, New York, 1977)
- [2] J. Kogut and L. Susskind, *Phys. Rev. D* 11 (1974) 395
- [3] S. Duane, A. D. Kennedy, B. J. Pendleton and D. Roweth, *Phys. Lett. B* 195 (1987) 216
- [4] N. A. Metropolis, N. M. Rosenbluth, A. H. Rosenbluth, E. Teller and J. Teller, *J. Chem. Phys.* 21 (1953) 1087
- [5] For a review of these methods in lattice QCD see A. Boriçi, *Krylov Subspace Methods in Lattice QCD*, PhD thesis, CSCS TR-96-27, ETH Zurich 1996
- [6] M. R. Hestenes and E. Stiefel, *J. Res. Nat. Bur. Stand.* 49 (1952) 409
- [7] W. E. Arnoldi, *Quart. Appl. Math.* 9 (1951) 17
- [8] Y. Saad and M. H. Schultz, *SIAM J. Sci. Stat. Comput.* 7 (1986) 856
- [9] H. A. Van der Vorst, *SIAM J. Sci. Stat. Comput.*, 13 (1992) 631
- [10] C. Lanczos, *J. Res. Nat. Bur. Stand.* 49 (1952) 33
- [11] P. H. Ginsparg and K. G. Wilson, *Phys. Rev. D* 25 (1982) 2649.
- [12] H. Neuberger, *Phys. Lett. B* 417 (1998) 141
- [13] A. Boriçi, *J. Comput. Phys.* 162 (2000) 123-131
- [14] C. F. Jagels und L. Reichel, *Num. Lin. Algeb. Appl.*, Vol. 1(6), 555-570 (1994)
- [15] A. Boriçi, in preparation.